Design of two-dimensional elliptically cylindrical invisible cloaks with multiple regions*

Luo Xiao-Yang(罗孝阳), Liu Dao-Ya(刘道亚), Liu Jin-Jing(刘锦景), and Dong Jian-Feng(董建峰)†

Department of Electronic Information Science and Technology, Ningbo University, Ningbo 315211, *China*

(Received 23 July 2013; revised manuscript received 29 September 2013; published online 25 March 2014)

Two-dimensional (2D) elliptically cylindrical invisible cloaks with multiple regions are designed based on the transformation optics and the complementary media theory. Multiple invisible cloak regions can be obtained by properly using the compressed or folded transformation in each space layer. The constitutive parameter tensor expressions for each region have been obtained. The results of full wave simulations by using finite element software confirm the validity of the constitutive parameter tensor expressions. In addition, the parameters are relatively easier to realize.

Keywords: transformation optics, complementary media theory, elliptically cylindrical invisible cloaks

PACS: 41.20.Jb, 42.25.Bs, 78.20.Bh **DOI:** 10.1088/1674-1056/23/5/054101

1. Introduction

In the past few years, invisible cloaks based on transformation optics and metamaterials have attracted extensive attention in the scientific and engineering communities. The theory of transformation optics was proposed by Pendry[1] and Leonhardt[2] independently, which is based on the form-invariant spatial coordinate transformations of Maxwell's equations. The first experimental demonstration of the cylindrical invisibility cloak at microwave frequency was realized by using metamaterials by Schurig *et al.*[3] Full-wave simulations of the cylindrical cloak and the calculation of the material properties for coordinate transformations have been presented by Cummer[4] and Schurig *et al.*[5] The interactions of electromagnetic waves with a general class of spherical cloaks were established analytically based on a full wave Mie scattering model by Chen *et al.*[6] The design of optical cloaks using metamaterials was reported by Cai *et al.*[7] Following these studies, a large number of papers on intensive investigation of invisibility cloaks based on transformation optics have been published.[8–17] Some review papers on transformation optics can be found, e.g., in Refs. [18]–[20].

Recently, a new class of cloak named the exterior cloak, which is different from the shell-like interior cloak,[1,3] has been proposed by Lai *et al.*[21] Based on a complementary media method and folded transformation optics, the exterior cloak can hide objects at a distance outside the cloaking shell. The key idea is a complementary "anti-object" embedded inside a shell with a "folded geometry".[21] The scattering of the object can be exactly eliminated by the "anti-object". The cloaked object can exchange information with the outer region because it lies outside the cloaking shell and can be seen. The external cloak with the parameters of permittivity and permeability homogeneously anisotropic, which can be realized easily in actual applications, has been proposed and validated by full-wave simulations.[22] The simplified circular[23] and elliptically[24] cylindrical external cloaks with only the axial material parameter spatially variant have been designed. More recently, cylindrical cloaks with multiple invisible regions and arbitrary polygonal cloaks with multiple invisible regions were reported by Luo *et al.*[25,26] The objects could be hidden in the interior cavity and exterior space simultaneously in one cloak with multiple invisible regions. In this paper, we investigate two-dimensional elliptically cylindrical invisible cloaks with multiple regions, which can be applied to hide objects in different areas. The constitutive parameter tensor expressions for each region have been derived. The results of full-wave simulations based on the finite-element software confirm the validity of the constitutive parameter tensors. Only the axial parameter of the cloak is spatially varied, and the transverse parameters are constants, which can be realized easily. This theoretical method can be used to design new invisible cloaks. This cloak provides more flexible choices for the objects to be hidden, which may be important in the applications of engineering such as wireless communication, etc.

2. Design method and constitutive parameter tensors

The schematic diagram for a two-dimensional (2D) elliptically cylindrical invisible cloak with multiple regions is shown in Fig. 1. The region surrounded by ξ_5 is the original space, and the boundaries of the elliptical-cylinder with the same focus from inside to outside are ξ_1, ξ_2, ξ_3, ξ_4, and ξ_5, re-

*Project supported by the National Natural Science Foundation of China (Grant No. 61078060), the Innovative Research Team Program of Ningbo, China (Grant No. 2009B21007), and the K.C. Wong Magna Fund in Ningbo University, China.

†Corresponding author. E-mail: dongjianfeng@nbu.edu.cn

© 2014 Chinese Physical Society and IOP Publishing Ltd

spectively. The material parameters can be obtained through a three-step coordinate transformation based on the transformation optics and the complementary media theory. Firstly, using folded transformation, the region $\xi_4 \le \xi \le \xi_5$ was transformed to region $\xi_3 \le \xi' \le \xi_4$. Secondly, the region $\xi_2 \le \xi \le \xi_3$ was transformed to region $\xi_1 \le \xi' \le \xi_2$. Thirdly, in order to rebuild a correct optical path, the region $0 \le \xi \le \xi_5$ was compressed to region $0 \le \xi' \le \xi_1$. It is known that the complementary media can "cancel" a certain space.[21] Hence, if objects placed in the regions $\xi_4 \le \xi' \le \xi_5$ and $\xi_2 \le \xi' \le \xi_3$, and the suitable "anti-object" is embedded in the corresponding complementary layer $\xi_3 \le \xi' \le \xi_4$ and $\xi_1 \le \xi' \le \xi_2$ respectively, the objects become invisible.

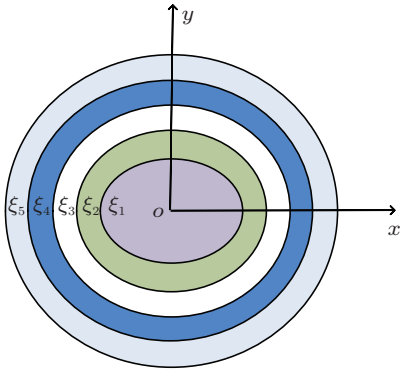


Fig. 1. (color online) Schematic of the 2D elliptically cylindrical invisible cloak with multiple regions.

By properly using a compressed or folded transformation, we can obtain cloaks with multiple invisible regions. This paper considers a two-dimensional elliptically cylindrical invisible cloak.

We adopt elliptically cylindrical coordinate system (ξ, η, z). The relationships between (ξ, η, z) and the Cartesian coordinates (x, y, z) are

$$\begin{cases} x = p\cosh\xi\cos\eta, \\ y = p\sinh\xi\sin\eta, \\ z = z, \end{cases} \tag{1}$$

where p is the semifocal length of the ellipse.

Choosing a proper transformation function, the original space was transformed to the transformation space based on folded transformation. The coordinate transformation function can be generally expressed as

$$\begin{cases} \xi' = f(\xi), \\ \eta' = \eta, \\ z' = z, \end{cases} \tag{2}$$

where f is a continuous function.

Based on the form invariant of the Maxwell equations and the transformation optics theory, the permittivity and permeability tensors in the transformation media are derived as

$$\varepsilon' = \Lambda\varepsilon\Lambda^{\mathrm{T}}/\det(\Lambda), \quad \mu' = \Lambda\mu\Lambda^{\mathrm{T}}/\det(\Lambda), \tag{3}$$

where Λ is the Jacobian transformation matrix with elements

$$\Lambda = \begin{bmatrix} f'h & 0 & 0 \\ 0 & h & 0 \\ 0 & 0 & 1 \end{bmatrix}, \tag{4}$$

where $h = \sqrt{\cosh 2\xi' - \cos 2\eta}/\sqrt{\cosh 2\xi - \cos 2\eta}$, f' is the derivative of f, $\det(\Lambda)$ is the determinant of the Jacobi matrix, and ε', μ', and ε, μ are the permittivity and permeability tensors of the transformation and the original space, respectively.

Firstly, the original spatial region $\xi_4 \le \xi \le \xi_5$ was transformed to the transformation spatial region $\xi_3 \le \xi' \le \xi_4$ based on folded transformation. The transformed function is chosen as

$$\begin{cases} \xi' = (\xi - \xi_4)(\xi_3 - \xi_4)/(\xi_5 - \xi_4) + \xi_4, \ \ \xi_4 \le \xi \le \xi_5, \\ \eta' = \eta, \ \ 0 \le \eta < 2\pi, \\ z' = z, \ \ z \in \mathbb{R}. \end{cases} \tag{5}$$

The nonlinear relationship between the coordinate parameters and the lengths of major axes r_i can be expressed as

$$\xi_i = \ln(r_i/p + \sqrt{(r_i/p)^2 - 1}), \ \ i = 1,2,3,4,5. \tag{6}$$

From Eqs. (3)–(5), we can obtain the relative permittivity and permeability tensors in outside transformed region ($\xi_3 \le \xi' \le \xi_4$) as

$$\begin{cases} \varepsilon'_{\xi'} = \mu'_{\xi'} = f'_1, \\ \varepsilon'_{\eta'} = \mu'_{\eta'} = \dfrac{1}{f'_1}, \\ \varepsilon'_{z'} = \mu'_{z'} = \dfrac{1}{f'_1}\dfrac{\cosh(2f_1^{-1}(\xi')) - \cos(2\eta')}{\cosh(2\xi') - \cos(2\eta')}, \end{cases} \tag{7}$$

where $f'_1 = (\xi_3 - \xi_4)/(\xi_5 - \xi_4)$, and $f_1^{-1}(\xi') = (\xi' - \xi_4)(\xi_5 - \xi_4)/(\xi_3 - \xi_4) + \xi_4$.

Then, the original spatial region $\xi_2 \le \xi \le \xi_3$ was transformed to the transformation spatial region $\xi_1 \le \xi' \le \xi_2$ using the following coordinate transformation function:

$$\begin{cases} \xi'' = (\xi - \xi_2)(\xi_1 - \xi_2)/(\xi_3 - \xi_2) + \xi_2, \ \ \xi_2 \le \xi \le \xi_3, \\ \eta'' = \eta, \ \ 0 \le \eta < 2\pi, \\ z'' = z, \ \ z \in \mathbb{R}. \end{cases} \tag{8}$$

From Eqs. (3), (4), and (8), the relative permittivity and permeability tensors in inner transformed region ($\xi_1 \le \xi' \le \xi_2$) can be obtained as

$$\begin{cases} \varepsilon''_{\xi''} = \mu''_{\xi''} = f'_2, \\ \varepsilon''_{\eta''} = \mu''_{\eta''} = \dfrac{1}{f'_2}, \\ \varepsilon''_{z''} = \mu''_{z''} = \dfrac{1}{f'_2}\dfrac{\cosh(2f_2^{-1}(\xi'')) - \cos(2\eta'')}{\cosh(2\xi'') - \cos(2\eta'')}, \end{cases} \tag{9}$$

where $f'_2 = (\xi_1 - \xi_2)/(\xi_3 - \xi_2)$, and $f_2^{-1}(\xi'') = (\xi'' - \xi_2)(\xi_3 - \xi_2)/(\xi_1 - \xi_2) + \xi_2$.

Finally, in order to rebuild the correct optical path, the total original space $0 \le \xi \le \xi_5$ should be restored in the interior

space $0 \le \xi' \le \xi_1$. The coordinate transformation function can be expressed as

$$\begin{cases} \xi''' = \xi\xi_1/\xi_5, \ \ 0 \le \xi \le \xi_5, \\ \eta''' = \eta, \ \ 0 \le \eta < 2\pi, \\ z''' = z, \ \ z \in \mathbb{R}. \end{cases} \tag{10}$$

From Eqs. (3), (4), and (10), the material parameters of the rebuilt media can be obtained as

$$\begin{cases} \varepsilon'''_{\xi'''} = \mu'''_{\xi'''} = \dfrac{\xi_1}{\xi_5}, \\ \varepsilon'''_{\eta'''} = \mu'''_{\eta'''} = \dfrac{\xi_5}{\xi_1}, \\ \varepsilon'''_{z'''} = \mu'''_{z'''} = \dfrac{\xi_5}{\xi_1} \dfrac{\cosh(2\xi_5\xi'''/\xi_1) - \cos(2\eta''')}{\cosh(2\xi''') - \cos(2\eta''')}. \end{cases} \tag{11}$$

Using this method, the cloaks have two regions to hide objects, one is the outside area ($\xi_4 \le \xi' \le \xi_5$) and the other is the inside area ($\xi_2 \le \xi' \le \xi_3$).

3. Simulation results and discussion

In this section, we present an example of an elliptically cylindrical invisible cloak with multiple regions and its full-wave simulations by using finite-element software to confirm the validity of the constitutive parameter tensors and the design method. The lengths of semimajor axes of ellipses from inside to outside are $a = 0.03$ m, $b = 0.04$ m, $c = 0.05$ m, $d = 0.06$ m, and $e = 0.07$ m, respectively. The semifocal length p is 0.02 m. The incident wave is a TM-mode plane wave with frequency $f = 6$ GHz. From our simulation, when this cloak works around this frequency, its cloaking performance is quite good; if the frequency of the incident wave is changed, the cloaking performance will be affected, and gradually becomes worse.

Firstly, we simulate the case where there are no objects and "anti-objects" embedded in the cloak shell. Figure 2 shows the simulation results. We can see that the cloak, without any concealed objects and "anti-objects", does not bring scattering, whenever the plan wave is incident from the x or y axis. That is to say, we will not find this cloak from its outside, so the cloak achieves a good camouflage effect. In order to further verify the validity of the permittivity and permeability tensors, more simulations were done. Figure 3 shows the results when the incident waves with different directions were applied to the cloak. From the outcomes, we know the magnetic field distributions of the cloak have no scattering, thus the system is invisible.

When a dielectric elliptical shell with $\varepsilon = 2$ and $\mu = 2$ is placed in the inner space ($\xi_2 \le \xi' \le \xi_3$), and the suitable "anti-object" is embedded in the corresponding complementary layer ($\xi_1 \le \xi' \le \xi_2$), the scattering pattern of the system is depicted in Fig. 4. Figure 4(a) shows the simulation result that a dielectric elliptical shell is placed in the space ($\xi_2 \le \xi' \le \xi_3$) and there is no "anti-object" embedded in the complementary layer. It can be found that the scattering exists distinctly,

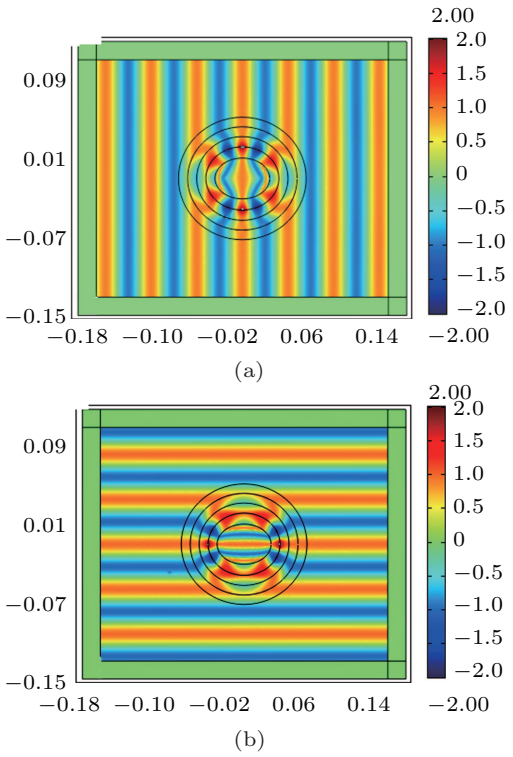


Fig. 2. (color online) Magnetic field distributions of elliptically cylindrical invisible cloaks with multiple regions. (a) The incident wave is along the x direction; (b) the incident wave is along the y direction.

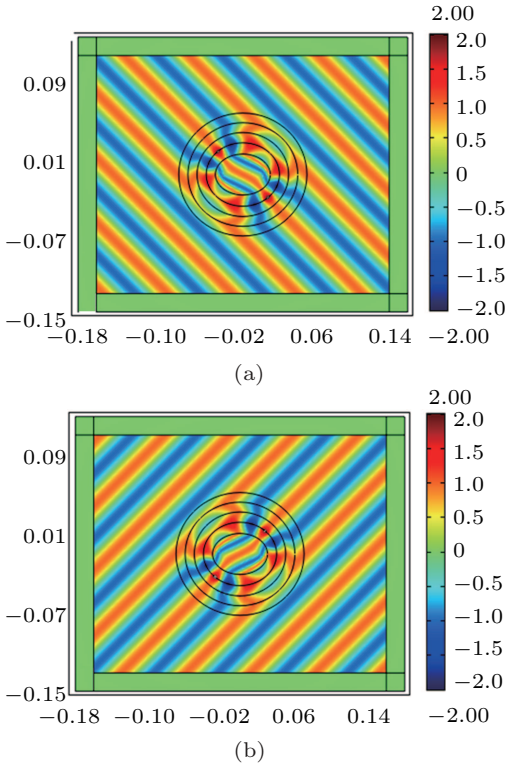


Fig. 3. (color online) Magnetic field distributions of elliptically cylindrical invisible cloaks with multiple regions when the plane wave irradiates obliquely.

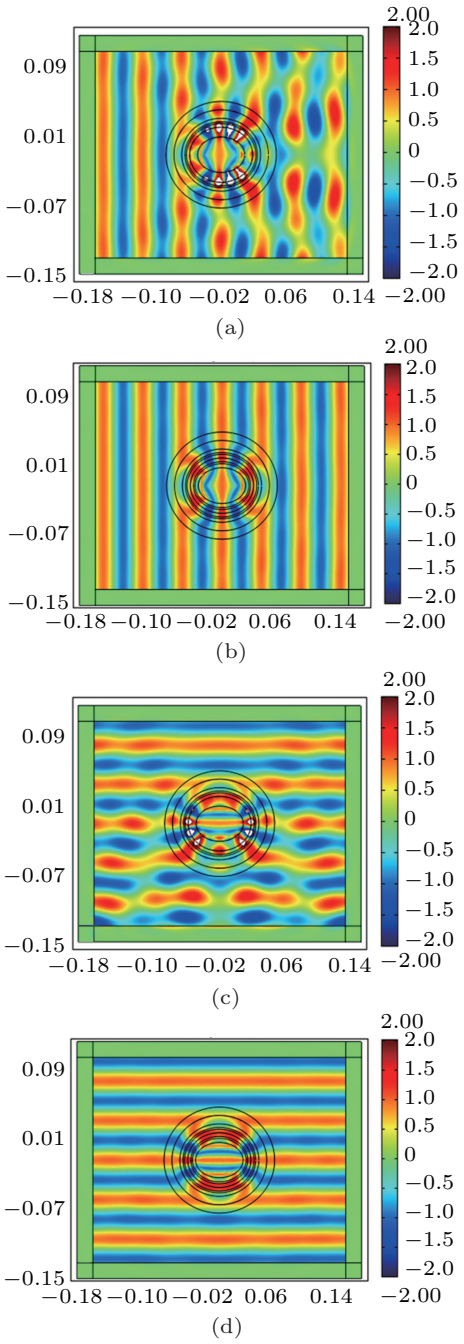


Fig. 4. (color online) Magnetic field distributions of the inner cloak region $\xi_2 \leq \xi' \leq \xi_3$. (a), (b) Under an incident TM wave along the x direction; (c), (d) under an incident TM wave along the y direction. (a), (c) The cloak embed object; (b), (d) the cloak embeded object and "anti-object".

which means that the cloak is still visible from the outside. Figure 4(b) shows the scattering pattern of the cloak, and the "anti-object" is embedded in the complementary layer. We can find the wave bends in the cloaking shells and fits to the fields outside the cloak smoothly. The scattering in Fig. 4(a) is now eliminated, and invisibility is achieved. Furthermore, we obtain the scattering distributions when the incident wave is from different directions. The large difference in the scattering patterns shown in Figs. 4(a) and 4(b) fully validates the cloaking effect of the inner cloak.

Similarly, in order to validate the cloaking effect of the outside region, a dielectric elliptical shell with $\varepsilon = 2$ and $\mu = 2$ is placed in the space $(\xi_4 \leq \xi' \leq \xi_5)$ and the suitable "anti-object" is embedded in the corresponding complementary layer $(\xi_3 \leq \xi' \leq \xi_4)$. The simulation results are shown in Fig. 5. Comparing with the cloak which does not embed the "anti-object", we can observe that the scattering pattern of the cloak with an "anti-object" still remains invisible. That is to say, the outside region $(\xi_4 \leq \xi' \leq \xi_5)$ can also be applied to hide objects.

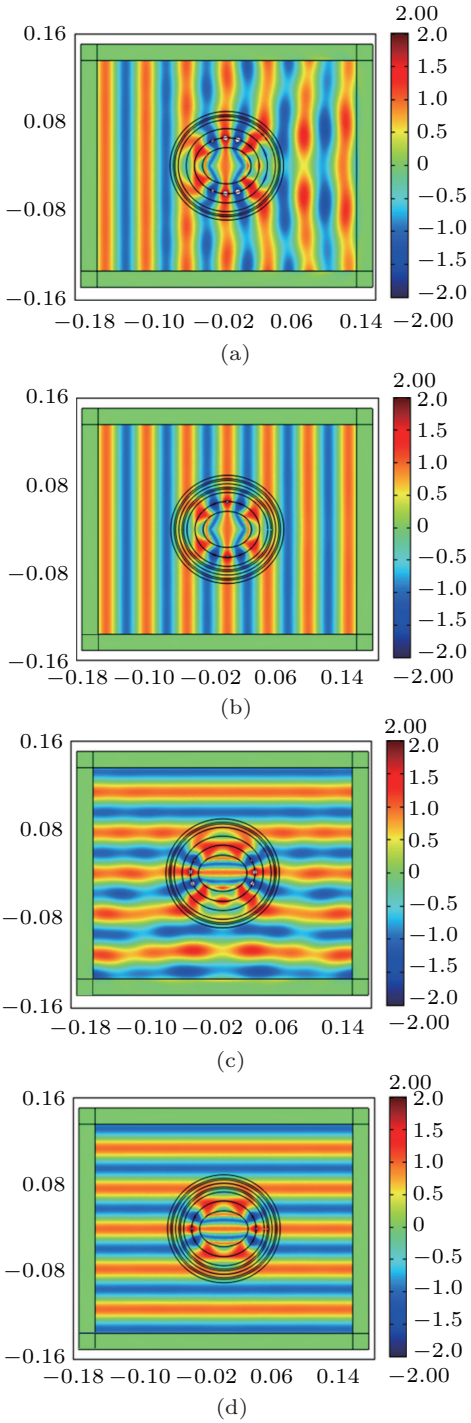


Fig. 5. (color online) Magnetic field distributions of the outside cloak region $\xi_4 \leq \xi' \leq \xi_5$. (a)–(d) The same as Fig. 4.

When two dielectric elliptical shells with $\varepsilon = 2$ and $\mu = 2$ are placed in the inner region ($\xi_2 \leq \xi' \leq \xi_3$) and the outside region ($\xi_4 \leq \xi' \leq \xi_5$) simultaneously, and the suitable "anti-objects" are embedded in the corresponding complementary layers, respectively, the simulation results show that the perfect scattering patterns of the whole system can be obtained for any incident wave's direction. Figures 6(a) and 6(b) show some simulation results, we can see that there is no scattering for the magnetic field distributions.

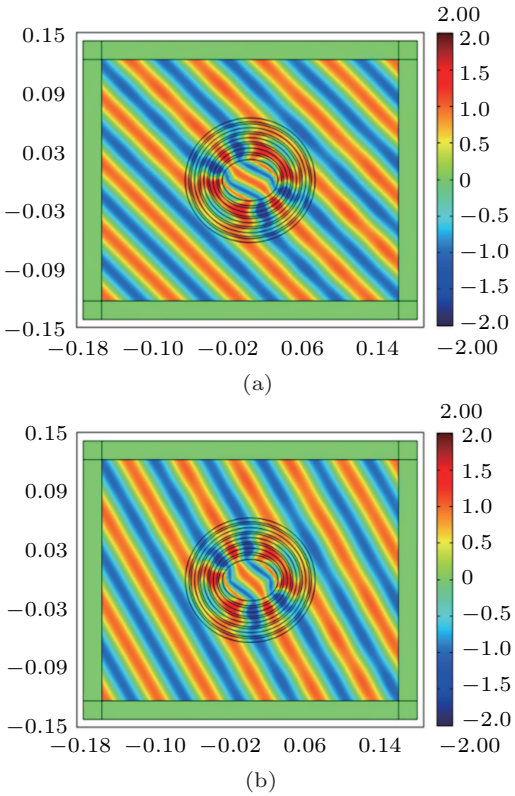


Fig. 6. (color online) Magnetic field distributions of the whole cloak model when the objects and "anti-objects" are placed in the inside and outside regions, respectively. (a) Under an incident TM wave along the 45° direction; (b) under an incident TM wave along the 30° direction.

When the value of p is close to zero, the elliptically cylindrical shell becomes a cylinder, and the simulation results are shown in Fig. 7. We can find that the magnetic field distributions are consistent with those of Ref. [25].

In Fig. 8, we show the electric field distributions of the cloak under an incident TE wave. From the simulation results, we can see that the cloaks are also suitable for a TE wave. Thus, this cloak can work for either a TE incident wave or a TM incident wave.

Finally, the constitutive parameter distributions of each transform region are presented in Fig. 9. We can see that the parameters of permittivity are constants as shown in Figs. 9(a), 9(b), 9(d), 9(e), 9(g), and 9(h). The varied parameter is the only permeability, as shown in Figs. 9(c), 9(f), and 9(i).

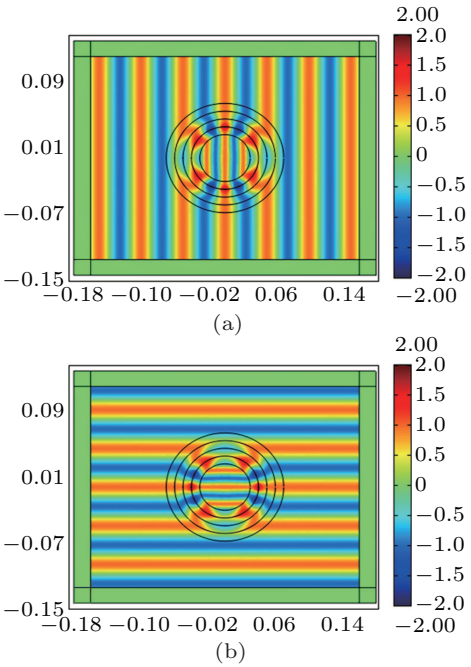


Fig. 7. (color online) Magnetic field distributions of the cylindrical cloak. (a) Under an incident TM wave along the x direction; (b) under an incident TM wave along the y direction.

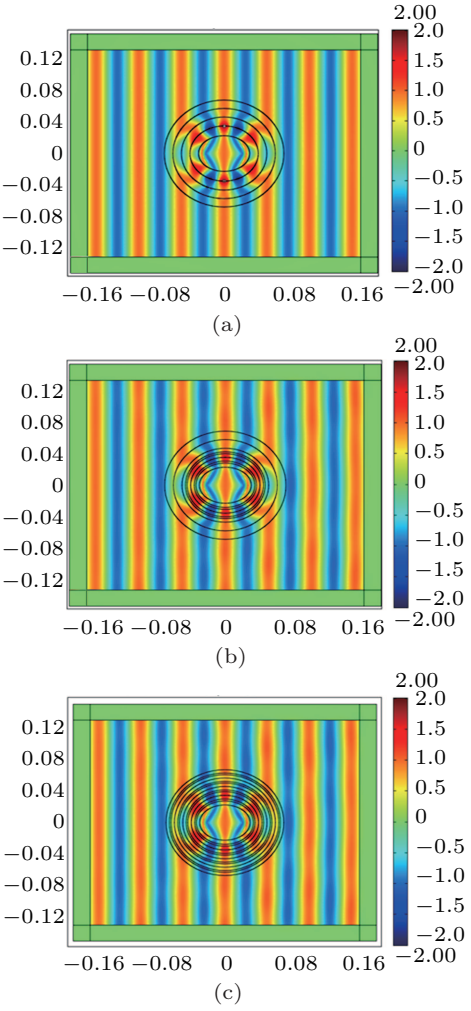


Fig. 8. (color online) Electric field distributions of the cloak under an incident TE wave. (a) There are no objects and "anti-objects". (b) The cloak of the inner region. (c) When the objects and "anti-objects" are placed in the inside and outside regions, respectively.

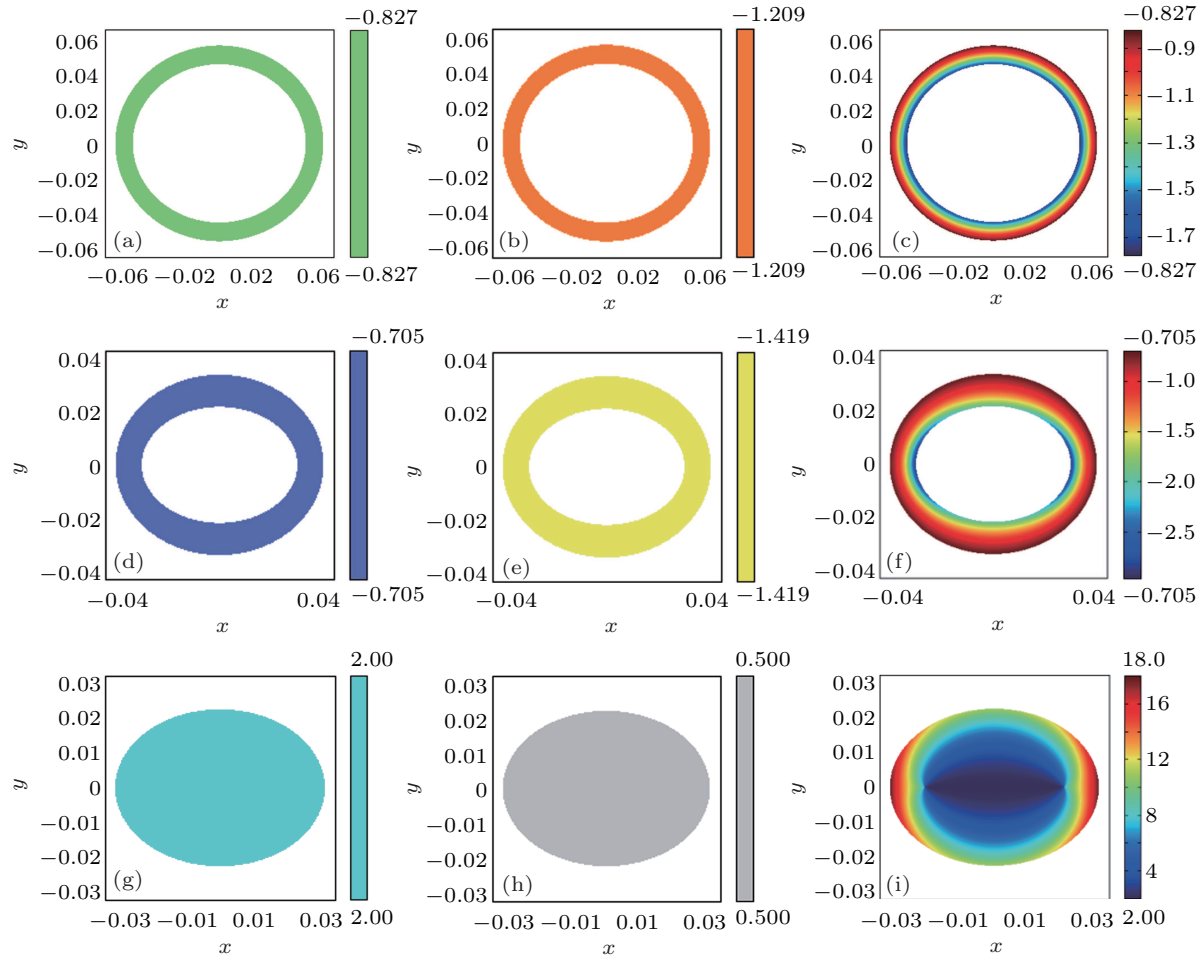


Fig. 9. (color online) Constitutive parameter distributions of the cloak. (a)–(c) The constitutive parameter of ε_η, ε_ξ, μ_z for region $\xi_3 \leq \xi' \leq \xi_4$, respectively. (d)–(f) The constitutive parameter of ε_η, ε_ξ, μ_z for region $\xi_1 \leq \xi' \leq \xi_2$, respectively. (g)–(i) The constitutive parameter of ε_η, ε_ξ, μ_z for region $0 \leq \xi' \leq \xi_1$, respectively.

4. Conclusion

Two-dimensional (2D) elliptical cylindrical invisible cloaks with multiple regions have been investigated in detail based on the transformation optics and the complementary media theory. We deduced the constitutive parameter tensor expressions for each region. The simulation results of the outside region, inner region and the whole model of the cloak have been obtained. The results of simulations confirm the validity of the constitutive parameter tensors, and the parameters are easy to realize in practical applications. The cloak with multiple invisible regions can be applied to hide objects in the inner and outside areas simultaneously. This work provides a new theoretical method for designing invisible cloaks.

References

[1] Pendry J B, Schurig D and Smith D R 2006 *Science* **312** 1780

[2] Leonhardt U 2006 *Science* **312** 1777

[3] Schurig D, Mock J J, Justice B J, Cummer S A, Pendry J B, Starr A F and Smith D R 2006 *Science* **314** 977

[4] Cummer S A, Popa B I, Schurig D, Smith D R and Pendry J B 2006 *Phys. Rev. E* **74** 036621

[5] Schurig D, Pendry J B and Smith D R 2006 *Opt. Express* **14** 9794

[6] Chen H, Wu B I, Zhang B and Kong J A 2007 *Phys. Rev. Lett.* **99** 063903

[7] Cai W, Chettiar U K, Kildishev A V and Shalaev V M 2007 *Nat. Photon.* **1** 224

[8] Luo Y, Chen H, Zhang J, Ran L and Kong J A 2008 *Phys. Rev. B* **77** 125127

[9] Jiang W X, Cui T J, Yu G X, Lin X Q, Cheng Q and Chin J Y 2008 *J. Phys. D: Appl. Phys.* **41** 085504

[10] Kwona D H and Werner D H 2008 *Appl. Phys. Lett.* **92** 013505

[11] Li C and Li F 2008 *Opt. Express* **16** 13414

[12] Ma H, Qu S, Xu Z, Zhang J, Chen B and Wang J 2008 *Phys. Rev. A* **77** 013825

[13] Ren C Y, Xiang Z H and Cen Z Z 2011 *Chin. Phys. B* **20** 114301

[14] Wu Q, Zhang K, Meng F Y and Li L W 2009 *J. Phys. D: Appl. Phys.* **42** 035408

[15] Gao D B and Zeng X W 2012 *Chin. Phys. Lett.* **29** 114302

[16] Li C and Li F 2008 *Opt. Express* **16** 13414

[17] Yang Y Q, Zhang M and Yue J X 2011 *Chin. Phys. B* **20** 024101

[18] Chen H, Chan C T and Sheng P 2010 *Nat. Mater.* **9** 387

[19] Kildishev A V and Shalaev V M 2011 *Phys. Usp.* **54** 53

[20] Liu Y and Zhang X 2012 *Nanoscale* **4** 5277

[21] Lai Y, Chen H Y, Zhang Z Q and Chan C T 2009 *Phys. Rev. Lett.* **102** 093901

[22] Han T C, Tang X H and Xiao F 2009 *J. Phys. D: Appl. Phys.* **42** 235403

[23] Li T, Huang M, Yang J, Yao Y and Yu J 2011 *Opt. Mat. Express* **1** 911

[24] Wang Z, Dong J F, Liu J J and Luo X Y 2012 *Acta Phys. Sin.* **61** 204101 (in Chinese)

[25] Luo Y, Zhu S Z, He L X and Wang Y 2011 *J. Opt.* **13** 015105

[26] Luo Y, He L X, Zhu S Z and Wang Y 2011 *J. Mod. Opt.* **58** 14